APPLICATIONS AND PERFORMANCE OF A NANORECEIVER WITH A CARBON NANOTUBE ANTENNA FOREST

C. EMRE KOKSAL AND EYLEM EKICI, THE OHIO STATE UNIVERSITY

ABSTRACT

We introduce an RF nanoreceiver, based on a forest of carbon nanotube (CNT) antennas packaged together. Based on the physical model of a charged carbon nanotube under RF exposure, which is significantly different from a typical RF antenna, we analyze the performance of our nanoreceiver. We show that, for low signal-bandwidth applications, our nanoreceiver is highly robust, allowing for continual operation over extended periods of time at low probabilities of error at reasonably low SNR values. For high signal-bandwidth applications, we show that at a given SNR, the achieved rate grows as $n^{1/4}$ with the number, n, of the CNTs, at reasonably low probabilities of error. Due to the extremely small scale of the CNTs, many millions of CNTs can be packed into very small areas (e.g., hundreds of millions in 1 mm^2) to achieve rates comparable to the commercially available wireless receivers. Hence, significant spatial miniaturization is achieved by our nanoreceiver compared to a classical RF receiver without a loss in the achievable rates.

INTRODUCTION

Nanoscale systems are envisioned for many crucial future applications ranging from targeted medicine and drug delivery to high fidelity sensors [1–5]. Miniaturization of communications systems has been in the forefront of research and development efforts for decades. Until very recently, communication system sizes and design alternatives were considered limited by the circuit, battery, but, most importantly, antenna sizes. For instance, the use of common operating frequencies of hundreds of megahertz to several gigahertz meant an antenna size on the order of centimeters. Such limitations render incorporation of communication into nanoscale systems impossible. Electromagnetic communication at such scales is reserved for the terahertz range, which has extremely high attenuation through matter [6]. Therefore, traditional EM-based communication had very limited use in nanoscale devices and systems. Instead, other paradigms were considered to facilitate communication of nanoscale devices for short distances [1, 7] via molecular communication, and longer distances [8, 9] via bacteria and nano-motors.

Recently, new EM-based radio receivers and transmitters have been proposed using carbon nanotubes (CNTs) [10, 11]. These communication systems are fundamentally different from traditional antenna-based systems: rather than relying on the oscillation of electrons inside the antenna in response to EM waves, CNTs oscillate themselves when they are charged. Oscillations lead to variation in the distance of the tip of the CNT from a cathode plate. The distance variations are then detected as fluctuations of the tunneling current. CNT-based receiver systems have been validated in implementation [10] and further analyzed in [12]. The ground-breaking property of CNT-based communication systems is that it is possible to establish communication from a few to hundreds of megahertz range with systems that are hundreds of nanometers in size. Even more recently, we have developed a communication-theoretical analysis of CNT-based receiver systems [13, 14]. Almost concurrently, system and networking aspects of nanoscale devices with CNT-based radios have been discussed in [15].

In this work, we analyze the behavior of forests of CNT antennas, which are composed of thousands or more CNTs vertically aligned on the same substrate. Using the unique response characteristics of charged CNTs under radio frequency (RF) exposure, we introduce two threads of analysis, highlighting two distinct use cases of CNT-based nano communication systems. For low signal-bandwidth applications, we show that our proposed receiver system is highly robust, allowing continual operation over extended periods of time with low probabilities of error at reasonably low signal-to-noise ratio (SNR) values. For the high signal-bandwidth applications, we show that the achieved rate grows as $n^{1/4}$ with the number, n, of the CNTs at reasonably low probabilities of error at a given SNR. Since CNT antennas can be packed very densely (e.g., hun-

1536-1284/12/$25.00 © 2012 IEEE

dreds of millions in 1 mm^2), significant spatial miniaturization is achieved by our nanoreceiver compared to a classical RF receiver without a loss in achievable rates.

Physical Model

The basic operation of the CNT-based nanoreceiver is illustrated in Fig. 1. It consists of a CNT attached to an anode with the other end free to move. CNTs behave like cantilevers with high elastic strength and an elastic constant in the 100 GPa range. A longitudinal electric field applied on a CNT induces a charge density at the tip of the CNT. Under electromagnetic excitation, the oscillating electric field perpendicular to the CNT exerts an oscillating force on it and causes it to move. Near the resonance frequency f_0 of the CNT cantilever, EM energy couples most efficiently into the CNT, and the CNT vibrates with a large amplitude. Fundamental properties such as mass, length, and diameter determine the resonance frequency and quality factor (Q) of the cantilever vibration. Overall, the resonance frequency is inversely proportional to the square of the length and the square root of the cross section area of the CNT. The response of the vibration amplitude to an oscillating electric field perpendicular to the CNT is proportional to

$$\frac{E_{rad}}{\sqrt{\left(f^2 - f_0^2\right)^2 + \left(f - f_0/Q\right)^2}},$$

where f_0 is the resonance frequency of the CNT, f_c and E_{rad} are the carrier frequency of the signal acting on the CNT and its amplitude, respectively, and Q is the quality factor. The response of the vibration amplitude peaks at $f = f_0$ and dies off rather fast as f moves "out of tune" from the resonance frequency f_0, as shown in Fig. 1. A simple theoretical model for electromagnetic excitation of CNTs is provided in [10].

The electric field between the free tip of the CNT and the cathode causes electrons to jump across the gap and results in *tunneling current*. The tunneling current varies exponentially with the distance between the tip and the cathode, governed by the Fowler Nordheim equation. Since the tunneling current depends exponentially on the inverse of the distance, small deviation of the CNT due to bending can lead to large changes in the tunneling current. The tunneling current resulting from the oscillation of the CNT has also been depicted in Fig. 1. Here, the variation in the current is proportional to the square of E_{rad} [10, 13] and is amplified by a factor, I_0, identical to the tunneling current observed when the CNT is at rest. This leads to a square-law behavior for the observed signal with respect to the incident radiant electric field strength.

Nanoreceiver Model

The block diagram of our nanoreceiver is illustrated in Fig. 2. The nanoreceiver is composed of two parts: the front-end and the energy detector. The basic components of the front-end summarize the physics of the charged CNTs under

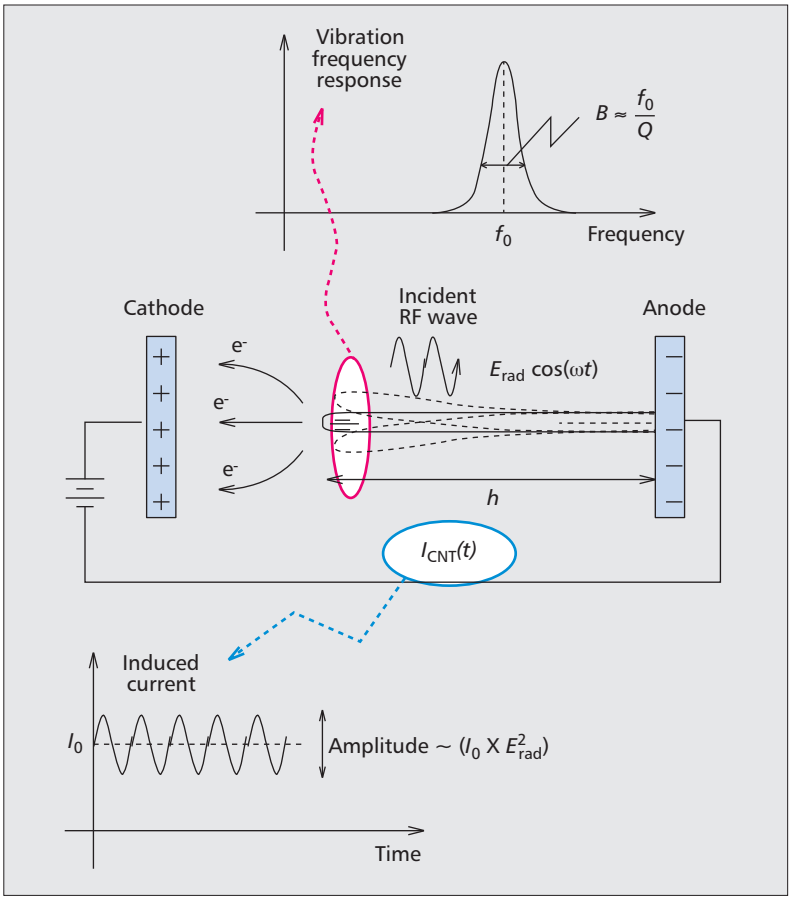

Figure 1. *Basic operation of a CNT receiver.*

an incident RF wave. The front-end includes n parallel CNT antennas and n associated square-law devices followed by an amplifier each. Here, $h_{CNT,j}(t)$ is the impulse response of the linear filter that captures the input-output behavior of the jth CNT antenna, where the input $s(t)$ is the electric field intensity of the incoming RF wave and the output $Y_{o,j}(t)$ is the amplitude of the associated vibrations in CNT j. The magnitude response of the jth CNT antenna is

$$H_{\mathrm{CNT},j}(f) = \left|\frac{Y_{o,j}(f)}{S(f)}\right| = \frac{q/m_{\mathrm{eff}}}{4\pi^2\sqrt{\left(f^2 - f_{c,j}^2\right)^2 + \left(ff_{c,j}/Q\right)^2}},$$

where $f_{c,j}$ is the resonance frequency of the jth CNT antenna, q is the charge at the tip, and m_{eff} is the effective mass of the CNT. We assume the length of each CNT antenna to be random. We model this randomness using a normal distribution, $f_{c,j} \sim \mathcal{N}(f_0, \sigma_{f_0}^2)$, independent of $f_{c,j'}$ for all $j' \uparrow j$. The 3 dB bandwidth, B, of the antenna response $H_{CNT,j}(f)$ can be found by solving $H_{CNT,j}(f_{c,j})/2 = H_{\mathrm{CNT},j}(f_{c,j} + B/2)$. With the additional assumption that the bandwidth is much smaller than the center frequency, $B \ll f_0$ (which is highly reasonable since the CNTs have a narrow pass-band), one can find $B \approx f_0/Q$ for all the CNTs.

Under both low signal-bandwidth and high signal-bandwidth regimes, we assume that the thresholds of the detector are chosen optimally to minimize the probability of error. Hence, we use maximum a posteriori or maximum likelihood decision rules.

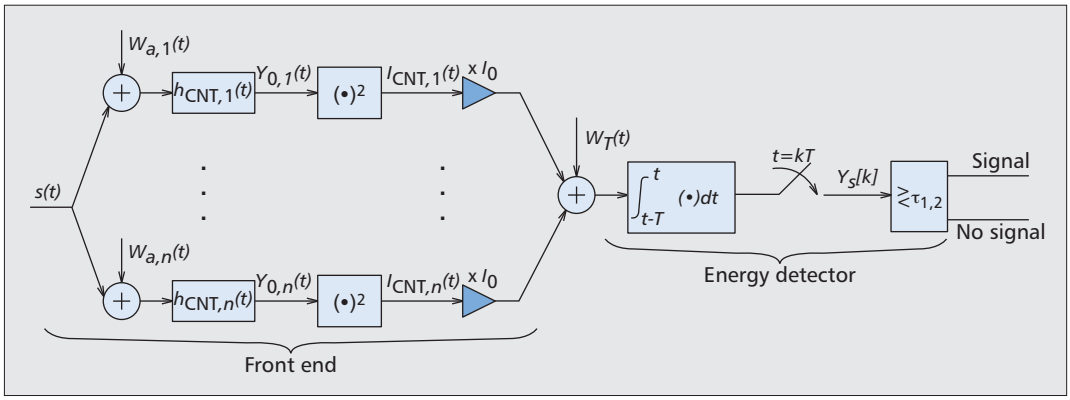

Figure 2. *System model of our nanoreceiver.*

We assume that the signal is corrupted by noise at two levels: *acoustic noise*, $W_{a,j}(t)$, is the mechanical component caused by radio static within the band of the antenna. Acoustic noise directly affects the amplitude of the vibrations $Y_{o,j}(t)$. The second one is *thermal noise*, $W_T(t)$, due to the electronic components of the detector and it is additive on the total detected current. We assume both the acoustic and thermal noise are additive white Gaussian. In our analysis, we assume that the acoustic noise is the dominant noise source for two reasons:

- The size of the CNT forest is large ($n \gg 1$) in our systems.
- Every branch of the front-end contains an amplifier with a very large gain (e.g., this gain is reported to be in the range of 50 dB in [10]).

The second component of the nanoreceiver is the energy detector. Since the signal $\sum_{j=1}^{n} I_{r,j}(t)$ is the current at the output of the front-end of the receiver, the integrator can be realized by a mere *capacitor*. The integrator is followed by the sampler, sampling the output of the integrator once every T s (symbol period); that is, the data rate is $1/T$ b/s. Each sample $Y_s[k]$ is compared to a pair of predetermined thresholds τ_1 and τ_2, and a 0 or 1 bit is decoded depending on these comparisons.

For information transmission, we assume that the simple on-off keying (OOK) signaling scheme is used. Apart from the simplicity of the scheme, there are other reasons that make OOK suitable for our nanoreceiver design. In OOK, during the ON period, the transmitter transmits pure sinusoids of duration T; thus, for each antenna j, we have $s(t) = a\cos(2\pi f_0 t + \phi)$, where ϕ is the random phase. Depending on the rate of information transmission desired by the application, the bandwidth of the input signal $s(t)$ can be large or small compared to the CNT bandwidth. The performance of our nanoreceiver under the low signal-bandwidth regime was studied in [14]. Here, we illustrate the performance under the high signal-bandwidth regime as well, and discuss the fundamental differences between the two.

The square-law device at each branch acts as a *demodulator* for the signal component (filtered by the antenna response $h_{CNT,j}(t)$) of each waveform $Y_{o,j}(t)$. This avoids the need for complicated components such as the phase locked loop to be implemented at the nano scale. The energy detector integrates $\sum_{j=1}^{n} (I_{CNT,j}(t)) + W_T(t)$ over T, and a sampler samples the output of the integrator every T s. Due to the square-law device, there are three components of $I_{CNT,j}(t)$ under the activation attempt: *signal component*; *signal-noise cross component*, which is a Gaussian process; and *noise-noise cross component*, which has Chi-squared samples. Under both low signal-bandwidth and high signal-bandwidth regimes, we assume that the thresholds of the detector are chosen optimally to minimize the probability of error. Hence, we use maximum a posteriori or maximum likelihood decision rules.

Applications and Performance

We consider two different types of applications, depending on the bandwidth of the RF signal. In the *low signal-bandwidth* regime, the signal bandwidth is much smaller than the bandwidth of the CNTs. Given that the typical CNT bandwidth varies between tens to hundreds of kilohertz [13], the low bandwidth regime allows for applications at rates lower than a few kilobits per second. The candidate applications include the activation of nanosystems, in which the system needs to remain inactive for a period of time and is expected to become active only when it receives an activation signal. The main performance goal in such applications is to simultaneously achieve low probabilities of false activation and unsuccessful activation. Consequently, the nanoreceiver can operate reliably over extended periods of time without observing an undesirable false activation, but becomes active correctly upon receiving an activation signal.

In the *high signal-bandwidth* regime, the signal bandwidth is much larger than the bandwidth of the CNTs. In this regime, our objective is to achieve data rates comparable to those of traditional RF receivers. We first analyze the achievable data rates as a function of the number of CNT antennas. Note that, due to extremely small scale of the CNTs, many millions of CNTs can be packed into very small areas (e.g., hundreds of millions in 1 mm^2). Exploiting this large number of CNT antennas, we show that it is possible to achieve data rates comparable to the commercially available wireless receivers at reasonably low bit error rates. Hence, a significant spatial miniaturization is achieved by our nanore-

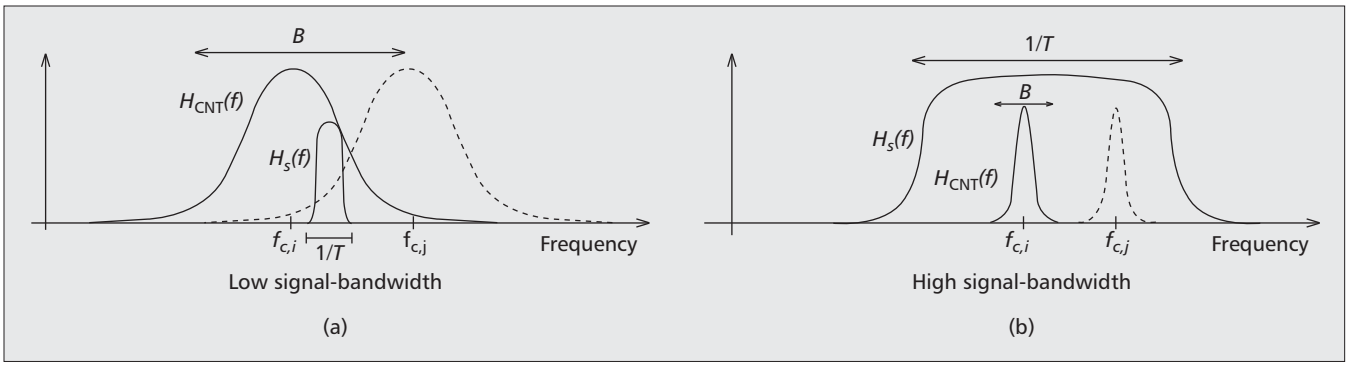

Figure 3. *Spectra of the signal and the CNT for high signal-bandwidth and low signal-bandwidth regimes.*

ceiver compared to a classical RF receiver without a loss in the achievable rates.

Low Signal-Bandwidth Regime — In this regime, we consider applications which do not require a high data rate, but a robust operation for extended amounts of time. In particular, in certain applications, nanosystems can be activated by activation signals sent remotely so that they initiate various tasks. For instance, nano-scale agents that are injected in human body can be used for targeted drug delivery. Once the activation signal is detected, they can release the drug. In such applications, the critical issue is the reliable operation for extended durations, rather than a high-data rate. Thus, in this regime, we assume the duration, T, of the activation signal to be large (i.e., $T >> 1/B$), where B is the bandwidth of a CNT.

The shapes of the spectra, $H_s(f)$ and $H_{CNT}(f)$, the activation signal, and a CNT, respectively, are illustrated in Fig. 3. There, one can see that the variations in the resonance frequency of the CNTs significantly affect the amount of signal energy that the system absorbs. As shown in Fig. 3, while the narrowband signal lies well in the band of CNT i, it is outside of the pass-band of CNT j, eliminating its contribution to the received energy.

To evaluate the performance of our nanoreceiver in the low signal-bandwidth regime, we analyze the probabilities of the error events. In particular, we evaluate p_{ua} and p_{fa}, which denote the probabilities of unsuccessful and false activation respectively. We also evaluate the overall probability of error, $p_e = p_a p_{ua} + (1 - p_a)p_{fa}$, where p_a denotes the probability of an activation signal in a given period of duration T. To find the error probabilities, we use the thresholds of our detector, corresponding to the maximum a posteriori (MAP) detection. We illustrate the associated performance in Fig. 4. There, the parameter values are $f_0 = 15$ MHz, $Q = 500$, which implies that the average CNT bandwidth $B = 30$ kHz. Also, activation probability is $p_a = 10^{-3}$, activation period length is $T = 0.1$ s, and the ratio of the standard deviation of the CNT lengths to the bandwidth is

$$\frac{\sigma_{f_0}}{B} = \frac{1}{3}.$$

In Fig. 4a, we plot the probability of error, p_e, as a function of the number of antennas for various values of SNR_a. It is notable that, even for a low SNR_a, it is possible to achieve low probabilities of error with a reasonably small number of CNTs. For instance, approximately $n = 1000$ CNTs is sufficient to achieve a p_e of 10^{-5}. Another important conclusion is that, the performance is highly sensitive to the variations of SNR_a. For instance, even to make up for a 1dB drop in SNR_a, we need to increase the number of CNTs by a factor of 100. While a certain SNR_a is sufficient to achieve a low error probability, a slight decrease in SNR_a causes a huge performance drop. This *phase-transition-like phenomenon* we observe in the error probability can be explained as follows. Due to the large number of CNTs, a substantial averaging of the acoustic noise occurs when the signals induced by the CNTs are combined at the output of the front-end. The cumulative noise, averaged over all the CNTs is almost deterministic. Thus, if the signal power is below that level, probability of error is high (with uncoded OOK modulation), but once the signal power exceeds that critical threshold, the probability of error becomes almost 0.

In Fig. 4b, we plot the receiver operating characteristics (ROC), that is, the trade-off between probabilities p_{ua} and p_{fa}. In this plot, the signal to acoustic noise ratio is $\text{SNR}_a = 0$dB. From the figure, one can deduce that $n = 3000$ CNTs is sufficient for *1 month of continual operation with* $p_{ua} = 10^{-7}$ *at a cumulative probability of false activation* $p_{fa} < 10^{-2}$ *over the entire month*. This example shows that the nanoreceiver can be highly reliable in the low signal-bandwidth regime, even with a few thousand CNTs.

High Signal-Bandwidth Regime — In this regime, our ultimate purpose is to use our nanoreceiver to achieve a data rate comparable to those achievable by traditional RF receivers. Since the bandwidth of a typical CNT is no more than a few hundreds of kilohertz, in this regime, the duration, T, of a symbol is much smaller than the CNT bandwidth: $T \ll 1/B$ at such data rates.

The shape of the spectra, $H_s(f)$ and $H_{CNT}(f)$, of a symbol and a CNT, respectively, are illustrated in Fig. 3. Each CNT has a relatively narrow bandwidth and, unlike the low bandwidth regime, will only absorb a small portion of the signal energy. In this regime, the signal spectrum is approximately constant along the range of resonance frequencies of CNTs. Thus, one can see that the variations in the resonance frequency of

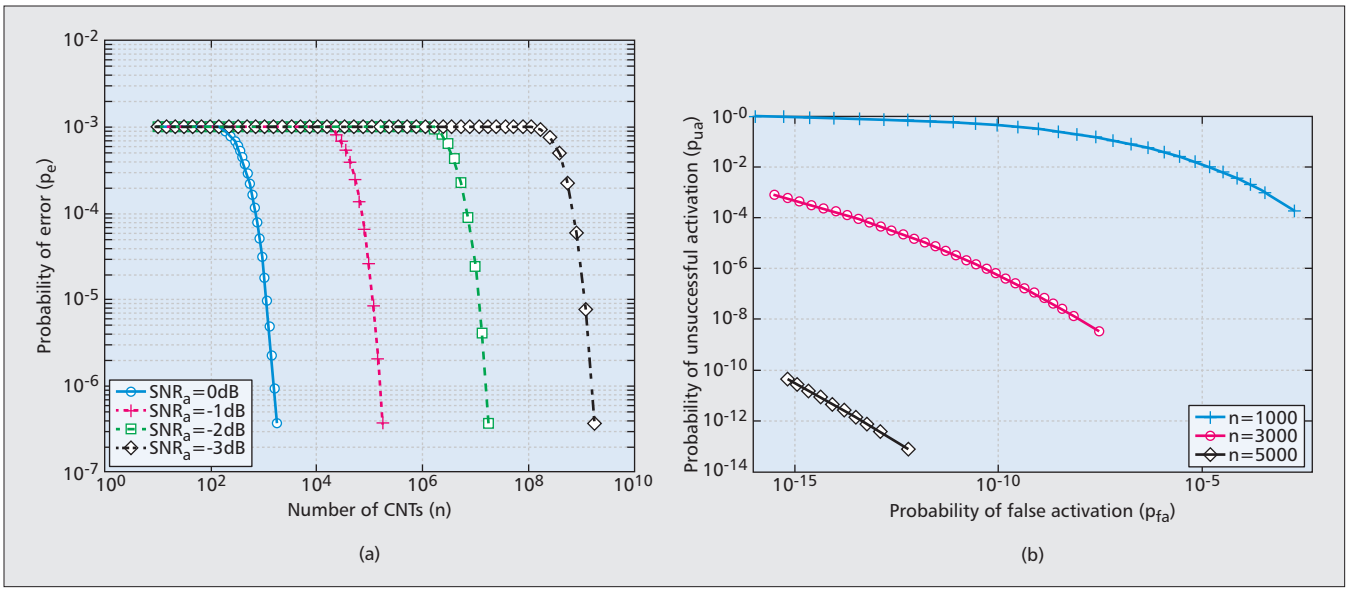

Figure 4. *Performance evaluation of the nanoreceiver in the low signalbandwidth regime: a) error probability vs. number of CNTs; b) receiver operating characteristics.*

the CNTs do not significantly affect the amount of signal energy each CNT absorbs.

To evaluate the performance of our nanoreceiver in the high signal-bandwidth regime, we analyzed the bit error rate (BER). Here, the data rate is $1/T$, and to evaluate the BER, we select the thresholds of our detector, corresponding to the maximum likelihood (ML) detection. We illustrate the associated performance in Fig. 5. There, the parameter values are $f_0 = 15$ MHz, $Q = 500$, which imply that the average CNT bandwidth is $B = 30$ kHz. The ratio of the standard deviation of the CNT lengths to the bandwidth is

$$\frac{\sigma_{f_0}}{B} = \frac{1}{3},$$

but since the signal bandwidth, $1/T \gg B$, the variation of the CNT resonance frequencies does not have any major impact on the performance.

In Fig. 5a, we plot the BER as a function of the number of CNTs at a data rate of 1 Mb/s (i.e., $T = 10^{-6}$). Here, the number of CNTs necessary to achieve similar performance to the low signal-bandwidth regime is significantly larger. Indeed, if we compare Fig. 5a with Fig. 4a, we can see that the same error probability at the same SNR value is achieved with a much larger number of CNTs in the high-bandwidth regime. This is plausible since, with the increase in rate (from low-bandwidth to high-bandwidth applications), most of the signal energy lies outside the pass-band of the CNT and gets filtered out. This loss in signal energy is made up for by the increase in the number of CNTs. However, the result is still optimistic, since the number of CNTs to achieve reasonable performance is feasible in the current state of nano-manufacturing technology. For instance, the size of the CNT forest necessary to achieve a BER of less than 10^{-6} at SNR$_a$ = –3 dB is $n = 10^6$, which can be planted in an area as small as 0.1 mm^2.

In Fig. 5b, we analyze the achievable data rate as a function of the number, n, of CNTs at a fixed bit error rate (BER). We illustrate the data rate as a function of the number of CNTs in Fig. 5b for a BER = 10^{-5} for various values of SNR$_a$. Note that, in this regime, the achieved rate grows as $n^{1/4}$ at a fixed BER. At reasonably low values of SNR, rates of order multiple megabits per second are achievable at a low BER. On the other hand, to increase the data rate by a factor of 2, we need roughly an order of magnitude increase in the number of CNTs. Thus, for a significant increase in the rate beyond the few megabits per second range, we need to either have a larger SNR or employ error control coding with more sophisticated modulation techniques than simple OOK. Indeed, from Fig. 5b, one can observe that a 3 dB coding gain gives us roughly a reduction factor of 5 in the number of CNTs at the data rate of 1 Mb/s.

Conclusions

We proposed a high-rate multi-CNT nanoreceiver and analyzed its performance. The proposed system is analyzed for two different application scenarios differentiated through the bandwidth of the received signal. Low signal-bandwidth scenarios are envisioned for applications requiring lower data rates, but a robust operation for very long operation durations. These systems are observed to undergo a phase-transition with increasing number of CNTs, where error rates drop almost to zero beyond scenario-specific thresholds. We also observe that it is possible to achieve very low error rates over months of operation time with only a few thousand CNTs. For the high signal-bandwidth scenarios, we envision the development of miniaturized receivers achieving data rates comparable to those achievable by traditional RF receivers. We show that high data rates and low error rates are achievable only through large numbers of CNTs, which are still plausible since millions of CNTs

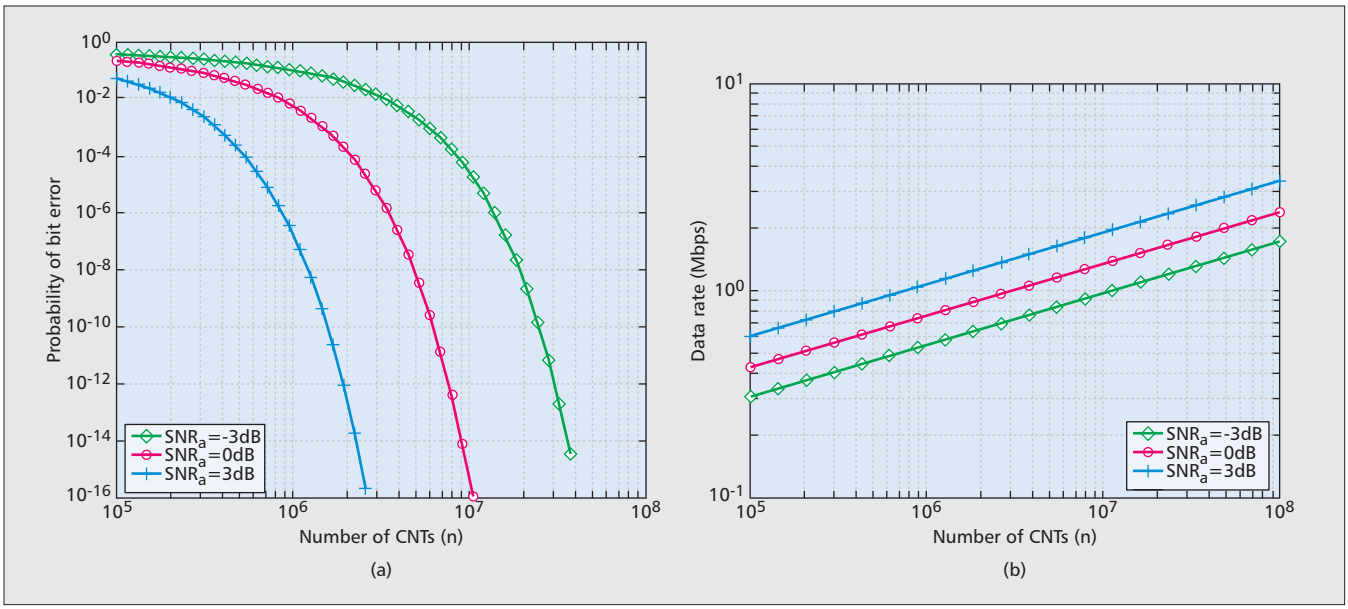

Figure 5. *Performance evaluation of the nanoreceiver in the high signalbandwidth regime: a) error probability vs. number of CNTs; b) data rate vs. the number of CNTs.*

can be planted in areas as small as fractions of a square millimeter . The data rate grows approximately proportional to the fourth root of the number of CNTs for a given bit error rate. Our results show that it is possible to achieve high reception rates at very small scales, paving the road toward a multitude of applications benefiting from the resulting miniaturization.

References

[1] I. Akyildiz and C. B. F. Brunetti, "Nanonetworks: A New Communication Paradigm," *Computer Networks*, vol. 52, 2008, pp. 2260–79.

[2] E. Drexler, *Nanosystems: Molecular Machinery, Manufacturing, and Computation*, Wiley, 1992.

[3] R. Freitas, "Nanotechnology, Nanomedicine and Nanosurgery," *Int'l. J. Surgery*, vol. 3, Nov. 2005, pp. 243–46.

[4] ——, "Pharmacytes: An Ideal Vehicle for Targeted Drug Delivery," *J. Nanoscience and Nanotechnology*, vol. 6, Sept. 2006, p. 2769–75.

[5] J. Aylott, "Optical Nanosensors an Enabling Technology for Intracelular Measurements," *Analyst*, 2003, pp. 309–12.

[6] J. M. Jornet and I. Akyildiz, "Channel Capacity of Electromagnetic Nanonetworks in the Terahertz Band," *Proc. IEEE ICC '10*, May 2010.

[7] M. Pierobon and I. Akyildiz, "A Physical End-to-End Model for Molecular Communication in Nanonetworks," *IEEE JSAC*, vol. 28, May 2010, pp. 602–11.

[8] M. Gregori and I. Akyildiz, "A New NanoNetwork Architecture using Flagellated Bacteria and Catalytic Nanomotors," *IEEE JSAC*, vol. 28, May 2010, pp. 612–19.

[9] B. Behkam and M. Sitti, "Bacterial Flagella-Based Propulsion and On/Off Motion Control of Microscale Objects," *Applied Physics Letters*, vol. 90, Jan. 2007.

[10] K. Jensen, J. Weldon, H. Garcia, and A. Zettl, "Nanotube Radio," *Nano Letters*, vol. 7, no. 11, Nov. 2007, pp. 3508–11.

[11] J. Weldon, K. Jensen, and A. Zettl, "Nanomechanical Radio Transmitter," *Physica Status Solidi B*, vol. 245, no. 10, Oct. 2008, pp. 2323–25.

[12] D. Dragoman and M. Dragoman, "Tunneling Nanotube Radio," *J. Applied Physics*, vol. 104, Oct. 2008.

[13] C. E. Koksal and E. Ekici, "A Nanoradio Architecture for Interacting Nanonetworking Tasks," *Elsevier Nano Commun. Networks J.*, vol. 1, Mar. 2010, pp. 63–75.

[14] C. E. Koksal, E. Ekici, and S. Rajan, "Design and Analysis of Systems Based on RF Receivers with Multiple Carbon Nanotube Antennas," *Elsevier Nano Commun. Networks J.*, vol. 1, no. 3, Sept. 2010, pp. 160–72.

[15] B. Atakan and O. B. Akan, "Carbon Nanotube-Based Nanoscale Ad Hoc Networks," *IEEE Commun. Mag.*, June 2010, pp. 129–35.

Biographies

C. Emre Koksal (koksal@ece.osu.edu) received his B.S. degree in electrical engineering from the Middle East Technical University, Ankara, Turkey, in 1996, and the S.M. and Ph.D. degrees from the Massachusetts Institute of Technology (MIT), Cambridge, in 1998 and 2002, respectively, in electrical engineering and computer science. He was a postdoctoral fellow in the Networks and Mobile Systems Group in the Computer Science and Artificial Intelligence Laboratory, MIT, and a senior researcher jointly in the Laboratory for Computer Communications and the Laboratory for Information Theory at EPFL, Lausanne, Switzerland. Since 2006 he has been an assistant professor in the Electrical and Computer Engineering Department, Ohio State University, Columbus. His general areas of interest are wireless communication, communication networks, information theory, stochastic processes, and financial economics. He is the recipient of the National Science Foundation CAREER Award (2011), the OSU College of Engineering Lumley Research Award (2011), and the co-recipient of an HP Labs Innovation Research Award. The paper he co-authored was a best student paper candidate at MOBICOM 2005.

Eylem Ekici [S'99, M'02, SM'11] (ekici@ece.osu.edu) received B.S. and M.S. degrees in computer engineering from Bogazici University, Istanbul, Turkey, in 1997 and 1998, respectively, and his Ph.D. degree in electrical and computer engineering from the Georgia Institute of Technology, Atlanta, in 2002. Currently, he is an associate professor with the Department of Electrical and Computer Engineering, Ohio State University. His current research interests include cognitive radio networks, vehicular communication systems, resource management, and analysis of network architectures and protocols. He is an Associate Editor of *Computer Networks Journal* (Elsevier), *ACM Mobile Computing and Communications Review*, and *IEEE/ACM Transactions on Networking*.